Research Article | Vol. 25, No. 12 | 12 June 2017 | OPTICS EXPRESS 13215
Optics EXPRESS

Pulse-spacing manipulation in a passively mode-locked multipulse fiber laser

YING YU,[1] XIAOMING WEI,[1,2,3] JIQIANG KANG,[1] BOWEN LI,[1] AND KENNETH K. Y. WONG[1,4]

[1]*Department of Electrical and Electronic Engineering, The University of Hong Kong, Pokfulam Road, Hong Kong*
[2]*Present address: Department of Medical Engineering, California Institute of Technology, 1200 East California Boulevard, Pasadena, California 91125, USA*
[3]*xmwei@eee.hku.hk*
[4]*kywong@eee.hku.hk*

Abstract: Passively mode-locked fiber lasers have been intensively applied in various research fields. However, the passive mode-locking typically operates in free-running regime, which easily produces messy multiple pulses due to the fruitful nonlinear effects involved in optical fibers. Actively controlling those disordered pulses in a passively mode-locked laser is of great interest but rarely studied. In this work, we experimentally investigate a flexible pulse-spacing manipulation in the passively mode-locked multipulse fiber laser by both intracavity and extracavity methods. A tuning range of pulse spacing up to 1.5 ns is achieved. More importantly, continuous pulse-spacing modulation is successfully demonstrated through external optical injection. It is anticipated that the results can contribute to the understanding of laser nonlinear dynamics and pursuing the optimal performance of passively mode-locked fiber lasers for practical applications.

OCIS codes: (140.0140) Lasers and laser optics; (140.3510) Lasers, fiber; (140.4050) Mode-locked lasers; (140.3538) Lasers, pulsed.

References and links

1. I. N. Duling, "All-fiber ring soliton laser mode locked with a nonlinear mirror," Opt. Lett. **16**(8), 539–541 (1991).
2. K. Tamura, E. P. Ippen, H. A. Haus, and L. E. Nelson, "77-fs pulse generation from a stretched-pulse mode-locked all-fiber ring laser," Opt. Lett. **18**(13), 1080–1082 (1993).
3. E. P. Ippen, C. V. Shank, and A. Dienes, "Passive mode locking of the cw dye laser," Appl. Phys. Lett. **21**(8), 348–350 (1972).
4. G. P. Agrawal, *Fiber-Optic Communiation Systems*, 3rd ed. (Wiley, 2002).
5. T. R. Schibli, K. Minoshima, F.-L. Hong, H. Inaba, A. Onae, H. Matsumoto, I. Hartl, and M. E. Fermann, "Frequency metrology with a turnkey all-fiber system," Opt. Lett. **29**(21), 2467–2469 (2004).
6. R. R. Gattass and E. Mazur, "Femtosecond laser micromachining in transparent materials," Nat. Photonics **2**(4), 219–225 (2008).
7. F. M. Mitschke and L. F. Mollenauer, "Discovery of the soliton self-frequency shift," Opt. Lett. **11**(10), 659–661 (1986).
8. M. Wanner, E. L. Tanzi, and T. S. Alster, "Fractional photothermolysis: treatment of facial and nonfacial cutaneous photodamage with a 1,550-nm erbium-doped fiber laser," Dermatol. Surg. **33**(1), 23–28 (2007).
9. C. Xu and F. W. Wise, "Recent advances in fibre lasers for nonlinear microscopy," Nat. Photonics **7**(11), 875–882 (2013).
10. C. W. Freudiger, W. Yang, G. R. Holtom, N. Peyghambarian, X. S. Xie, and K. Q. Kieu, "Stimulated Raman scattering microscopy with a robust fibre laser source," Nat. Photonics **8**(2), 153–159 (2014).
11. B. E. Bouma, L. E. Nelson, G. J. Tearney, D. J. Jones, M. E. Brezinski, and J. G. Fujimoto, "Optical coherence tomographic imaging of human tissue at 1.55 μm and 1.81 μm using Er-and Tm-doped fiber sources," J. Biomed. Opt. **3**(1), 76–79 (1998).
12. P. Grelu and N. Akhmediev, "Dissipative solitons for mode-locked lasers," Nat. Photonics **6**(2), 84–92 (2012).
13. D. R. Solli, C. Ropers, P. Koonath, and B. Jalali, "Optical rogue waves," Nature **450**(7172), 1054–1057 (2007).
14. C. Lecaplain, P. Grelu, J. M. Soto-Crespo, and N. Akhmediev, "Dissipative Rogue Waves Generated by Chaotic Pulse Bunching in a Mode-Locked Laser," Phys. Rev. Lett. **108**(23), 233901 (2012).
15. C. Lecaplain and P. Grelu, "Rogue waves among noiselike-pulse laser emission: An experimental investigation," Phys. Rev. A **90**(1), 013805 (2014).

#290168 https://doi.org/10.1364/OE.25.013215
Journal © 2017 Received 3 Apr 2017; revised 19 May 2017; accepted 20 May 2017; published 1 Jun 2017

Optics EXPRESS

16. A. F. J. Runge, C. Aguergaray, N. G. R. Broderick, and M. Erkintalo, "Raman rogue waves in a partially mode-locked fiber laser," Opt. Lett. **39**(2), 319–322 (2014).
17. M. Liu, A. P. Luo, W. C. Xu, and Z. C. Luo, "Dissipative rogue waves induced by soliton explosions in an ultrafast fiber laser," Opt. Lett. **41**(17), 3912–3915 (2016).
18. A. F. J. Runge, N. G. R. Broderick, and M. Erkintalo, "Observation of soliton explosions in a passively mode-locked fiber laser," Optica **2**(1), 36–39 (2015).
19. M. Liu, A. P. Luo, Y. R. Yan, S. Hu, Y. C. Liu, H. Cui, Z. C. Luo, and W. C. Xu, "Successive soliton explosions in an ultrafast fiber laser," Opt. Lett. **41**(6), 1181–1184 (2016).
20. S. Chouli and P. Grelu, "Rains of solitons in a fiber laser," Opt. Express **17**(14), 11776–11781 (2009).
21. W. Chang, A. Ankiewicz, J. M. Soto-Crespo, and N. Akhmediev, "Dissipative soliton resonances," Phys. Rev. A **78**(2), 023830 (2008).
22. E. Ding, P. Grelu, and J. N. Kutz, "Dissipative soliton resonance in a passively mode-locked fiber laser," Opt. Lett. **36**(7), 1146–1148 (2011).
23. X. Wu, D. Y. Tang, H. Zhang, and L. M. Zhao, "Dissipative soliton resonance in an all-normal-dispersion erbium-doped fiber laser," Opt. Express **17**(7), 5580–5584 (2009).
24. Z. C. Luo, W. J. Cao, Z. B. Lin, Z. R. Cai, A. P. Luo, and W. C. Xu, "Pulse dynamics of dissipative soliton resonance with large duration-tuning range in a fiber ring laser," Opt. Lett. **37**(22), 4777–4779 (2012).
25. D. Y. Tang, L. M. Zhao, B. Zhao, and A. Q. Liu, "Mechanism of multisoliton formation and soliton energy quantization in passively mode-locked fiber lasers," Phys. Rev. A **72**(4), 043816 (2005).
26. Y. Xu, Y. Song, G. Du, P. Yan, C. Guo, G. Zheng, and S. Ruan, "Soliton dynamic patterns of a passively mode-locked fber laser operating in a 2μm region," Laser Phys. Lett. **12**(4), 045108 (2015).
27. X. Wei, Y. Xu, S. Tan, S. Xu, Z. Yang, K. K. Tsia, and K. K. Y. Wong, "Pulsing Manipulation in a 1.55-μm Mode-Locked Fiber Laser by a 1-μm Optical Pattern," IEEE Photonics Technol. Lett. **27**(18), 1949–1952 (2015).
28. A. Niang, F. Amrani, M. Salhi, H. Leblond, A. Komarov, and F. Sanchez, "Harmonic mode-locking in a fiber laser through continuous external optical injection," Opt. Commun. **312**, 1–6 (2014).
29. F. Amrani, A. Haboucha, M. Salhi, H. Leblond, A. Komarov, and F. Sanchez, "Dissipative solitons compounds in a fiber laser. Analogy with the states of the matter," Appl. Phys. B **99**(1), 107–114 (2010).
30. S. Chouli and P. Grelu, "Soliton rains in a fiber laser: An experimental study," Phys. Rev. A **81**(6), 063829 (2010).
31. F. Sanchez, P. Grelu, H. Leblond, A. Komarov, K. Komarov, M. Salhi, A. Niang, F. Amrani, C. Lecaplain, and S. Chouli, "Manipulating dissipative soliton ensembles in passively mode-locked fiber lasers," Opt. Fiber Technol. **20**(6), 562–574 (2014).
32. W. H. Loh, A. B. Grudinin, V. V. Afanasjev, and D. N. Payne, "Soliton interaction in the presence of a weak nonsoliton component," Opt. Lett. **19**(10), 698–700 (1994).
33. D. Y. Tang, W. S. Man, and H. Y. Tam, "Stimulated soliton pulse formation and its mechanism in a passively mode-locked fibre soliton laser," Opt. Commun. **165**(4-6), 189–194 (1999).
34. F. M. Mitschke and L. F. Mollenauer, "Experimental observation of interaction forces between solitons in optical fibers," Opt. Lett. **12**(5), 355–357 (1987).
35. J. P. Gordon and H. A. Haus, "Random walk of coherently amplified solitons in optical fiber transmission," Opt. Lett. **11**(10), 665–667 (1986).
36. D. Y. Tang, B. Zhao, L. M. Zhao, and H. Y. Tam, "Soliton interaction in a fiber ring laser," Phys. Rev. E Stat. Nonlin. Soft Matter Phys. **72**(1), 016616 (2005).
37. M. Stratmann, T. Pagel, and F. Mitschke, "Experimental observation of temporal soliton molecules," Phys. Rev. Lett. **95**(14), 143902 (2005).
38. A. N. Pilipetskii, E. A. Golovchenko, and C. R. Menyuk, "Acoustic effect in passively mode-locked fiber ring lasers," Opt. Lett. **20**(8), 907–909 (1995).
39. J. K. Jang, M. Erkintalo, S. G. Murdoch, and S. Coen, "Ultraweak long-range interactions of solitons observed over astronomical distances," Nat. Photonics **7**(8), 657–663 (2013).

1. Introduction

Among the technologies for short pulse generation, passive mode-locking via fiber optics is advanced for the low cost, small footprint and easy maintenance [1,2], particularly in contrast to its solid-state counterpart [3]. Its capacities of wide wavelength tuning range and high peak power have largely benefited plenty of scientific and industrial applications, such as optical communication [4], frequency metrology [5], nanomaterial processing [6], self-frequency shifting wave generation [7], as well as clinical diagnosis and treatment [8]. Recently, tailor-made passively mode-locked fiber lasers have also been widely applied to biological imaging, examples including multiphoton microscopy [9], coherent Raman spectroscopy [10] and optical coherent tomography [11]. Despite of its superior robustness, passive mode-locking is a dissipative process involving composite mechanisms and effects, e.g., nonlinearity, dispersion, loss and gain [12]. Such a complex system, indeed, is an ideal platform for

Optics EXPRESS

nonlinear physics study, which has gained its popularity in the past few years, e.g., optical rogue wave generation [13–17], soliton explosion [18,19], soliton rain [20], and soliton resonance [21–24]. Therein, the randomly-arranged multiple pulses arising from peak power clamping [25], on the other hand, make the control and understanding of nonlinear physics involved in the passive mode-locking more difficult. Consequently, manipulating the multiple pulses in a passively mode-locked fiber laser is technically interesting for stabilizing its performance and unveiling the mystery behind the laser dynamics. However, the passively mode-locked fiber laser is a self-organized all-optical system, which makes the internal electronic control difficult by itself. On the other hand, all-optical technology can be a potential alternative solution, which unfortunately has been rarely investigated [26–31]. In this work, we experimentally demonstrate an all-optical pulse-spacing manipulation in a passively mode-locked multipulse fiber laser by both intracavity and extracavity methods. The results not only show the potential for precise control of the multipulse dynamics for optimal performance, but are also instructive for understanding the physics of the nonlinear laser dynamics.

2. Experimental setup

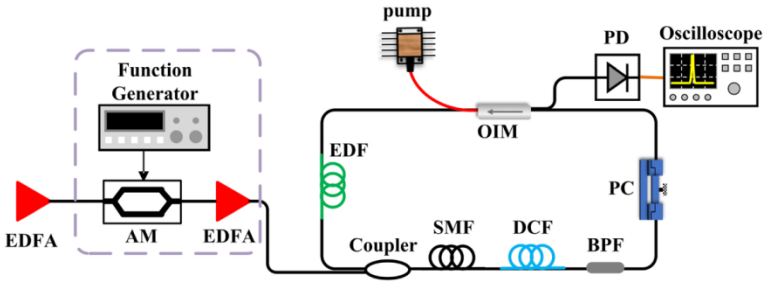

Fig. 1. Experimental setup. **EDFA**, erbium-doped fiber amplifier; **AM**, amplitude modulator; **OIM**, optical integrated module; **EDF**, erbium-doped fiber; **SMF**, single-mode fiber; **DCF**, dispersion-compensating fiber; **BPF**, band-pass filter; **PC**, polarization controller; **PD**, photodetector.

Figure 1 shows the overview of experimental setup. It includes two parts, external optical signal generator and passively mode-locked fiber cavity. The fiber cavity was passively mode-locked through nonlinear polarization rotation (NPR) mechanism in a ring configuration. An optical integrated module (OIM) composed of wavelength-division multiplexing, polarization-sensitive isolation and optical coupling was used to loop the ring cavity. A 980-nm pump laser (II-VI LC96AA74P-20) was injected into the fiber cavity through OIM and forward pumped a gain fiber, i.e., a 0.6-m erbium-doped fiber (EDF, Thorlabs ER80-8/125) with dispersion parameter of 15.6 ps/(nm•km). The polarization-sensitive isolation provided by OIM enabled the unidirectional operation and polarization-dependent loss for pulse narrowing, which plays an important role in NPR mode-locking. The polarization state of lightwave inside the fiber cavity was controlled by an in-line polarization controller (PC). The optical signal was extracted from the fiber cavity through the tap port of OIM (10%) for characterization. A 4-nm band-pass filter (BPF) with a center wavelength of 1540 nm was employed to confine the wavelength of mode-locking. The total cavity length was 38.1 m, mainly made of a single-mode fiber (SMF, 35.5 m) and a dispersion-compensating fiber (DCF, 2.0 m) with dispersion parameter of −81.3 ps/(nm•km). The corresponding fundamental repetition rate was 5.4 MHz, and the net cavity dispersion was −0.53 ps^2, which is a large anomalous dispersion that typically supports the soliton generation. The output optical signal was detected by a 15-GHz photodetector (PD, HP 11982A). Subsequently, it was digitized and recorded by a real-time oscilloscope (Lecroy SDA 820Zi-B) with 20-GHz bandwidth and 80-GS/s sampling rate. To perform external

Optics EXPRESS

optical control, a fiber coupler was used for coupling the external control signal into the passively mode-locked fiber laser. The external control signal was provided by an amplified spontaneous emission (ASE) source (i.e., a non-seeded EDFA). To demonstrate the external modulation of pulse spacing, the intensity of ASE was modulated by an amplitude modulator (AM) driven by a function generator. Another EDFA was utilized to compensate the insertion loss introduced by the AM.

The mode-locking was self-started by simply increasing the pump power. Owing to the nonlinear nature, the passively mode-locked fiber laser was turned into multipulse mode-locking when the pump power was further appropriately increased. At a pump power of >132.1 mW, the mode-locked laser operated in a dual-pulse state. Figure 2(a) shows its optical spectrum measured by an optical spectrum analyzer (OSA), while its pulse train measured by the real-time oscilloscope is shown in Fig. 2(b). The dual-pulse train has a period of 186.7 ns and there are two pulses in the same round trip. It should be pointed out that, harmonic mode-locking with equal pulse spacing can be obtained through dedicatedly tuning the PC, not shown here. In order to perform a long-term observation in the following experiments, the real-time oscilloscope was set to the auto-save mode at a frame rate of about 59 frame/s, and was triggered by the rising edge of the first pulse.

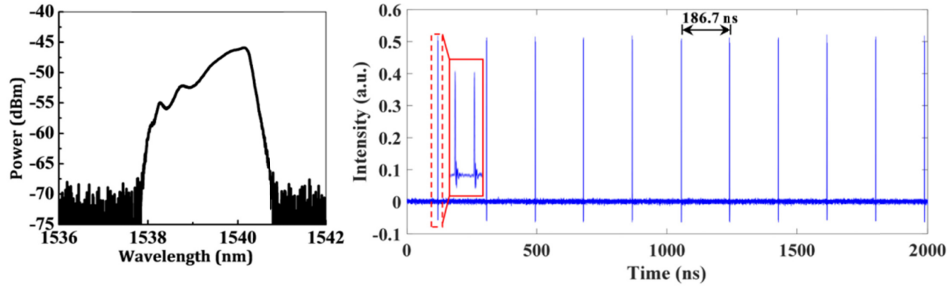

Fig. 2. (a) The optical spectrum of passively mode-locked fiber laser. (b) A typical time-domain dual-pulse train.

3. Pulse-spacing manipulation by controlling pump power

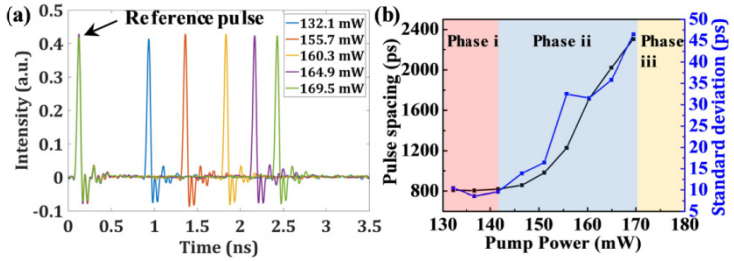

Fig. 3. The pulse spacing as a function of intracavity pump power. (a) Pulse waveforms. (b) Average pulse spacing and standard deviation.

At a pump power of 132.1 mW, the dual-pulse spacing was 809 ps. Increasing from this pump level, the dual-pulse spacing can be monotonously increased. Figure 3(a) shows an assembly of dual-pulse waveform snapshots at different pump powers. The first pulse was overlapped in the same temporal position as a reference pulse, and it is obvious that the dual-pulse spacing monotonically increases with the pump power. In order to statistically explore the trend of dual-pulse spacing via changing the pump power, 20000 frames were captured for different pump power levels, and the means and standard deviations of dual-pulse spacing were calculated. As shown in Fig. 3(b), the variation of dual-pulse spacing can approximately

Optics EXPRESS

be classified into three phases. From 132.1 mW to 141.6 mW, the dual-pulse spacing almost remains unchanged, while for a pump power higher than 141.6 mW, the dual-pulse spacing however increases with the pump power. It is noted that the increasing dual-pulse spacing can only sustain within a certain pump range, i.e., lower than 169.5 mW in this case, beyond that another one or even more pulses can be generated. This matches well with the finding of soliton energy quantization in a passively mode-locked fiber laser [25]. In the second phase, i.e., from 141.6 mW to 169.5 mW, the standard deviation of dual-pulse spacing would increase with the pump power. According to the curve of Fig. 3(b), the pulse spacing between the coexisting pulses can be flexibly controlled by changing the pump power. The physical mechanism behind can be understood as follows: the increasing pump power enhances the coexisting nonsoliton wave and as well as interaction between the solitons and nonsoliton wave [32, 33]. It is clearly shown in Fig. 3(a) that, the soliton intensity is almost unchanged as the pump power increases, which means that the energy of a higher pump does not correspondingly transform to the energy of solitons due to the soliton energy quantization effect [25], but to the nonsoliton background instead, i.e., enhancing the non-soliton background. This enhancing nonsoliton wave subsequently changes the soliton central wavelength (i.e., the carrier frequency) and thus induces temporal shift in a sufficient circulating time. Furthermore, the amount of temporal shift between the initial and final stationary states is monotonously increased with the amplitude of nonsoliton-wave [32].

4. Pulse-spacing manipulation by ASE injection

In addition to the intracavity control via pump power, it should also be technically interesting to manipulate the pulse spacing through external parameters. Herein, we further exploit the pulse spacing manipulation through external optical injection. The external optical source was a cost-effective ASE source. As we discussed in the intracavity scheme, a higher pump power can separate the two pulses farther apart due to the enhancement of nonsoliton perturbation. On the other hand, an externally injected ASE signal can also impact on the pulse spacing. The utilization of ASE noise source is based on another consideration that, rather than other CW sources, the relatively weak in-band intensity of ASE signal is not that easy to destroy a passive mode-locking operation.

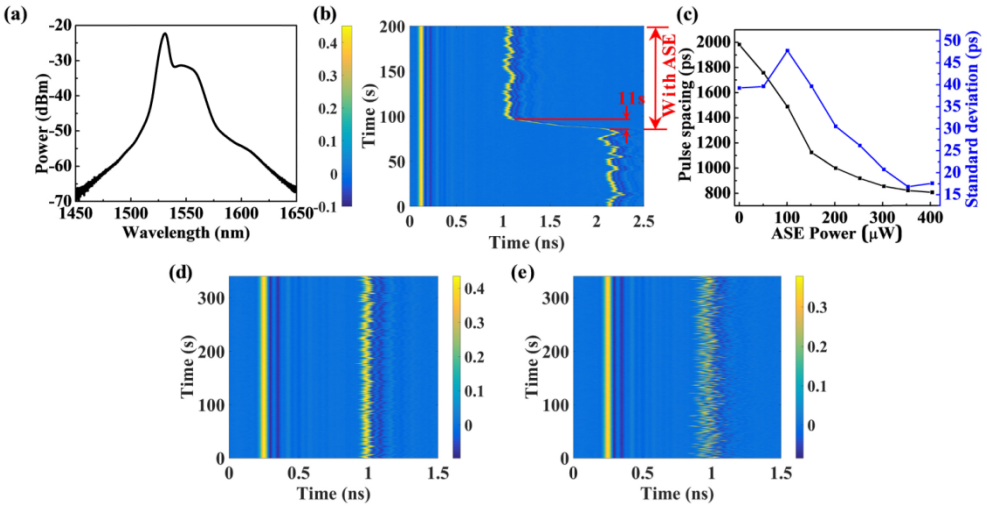

Fig. 4. (a) The optical spectrum of the injected ASE signal. (b) The pulse spacing evolution with ASE injection. (c) The pulse spacing as a function of injected ASE power. (d) and (e) are pulse spacing evolution with different ASE powers: (d) is corresponding to a smaller ASE power of 351 μW, while (e) is corresponding to a larger ASE power of 1660 μW.

Optics EXPRESS

The typical optical spectrum of the ASE noise from an EDFA is shown in Fig. 4(a). It was injected into the fiber cavity through a coupler. Figure 4(b) shows how dual-pulse spacing changes after ASE injection. At the beginning, the dual-pulse spacing was about 2.0 ns. After injecting a 202-μW ASE signal into the cavity, the dual-pulse spacing became smaller and smaller, until ~1.0 ns, and the corresponding transition time is about 11 s. In order to explore the relationship between the stationary dual-pulse spacing and injected ASE power, similar calculation as in Fig. 3(b) was performed and shown in Fig. 4(c). It should be pointed out that, the dual-pulse spacing was initially set to 2.0 ns via pump power for every injection case of Fig. 4(c). As can be observed, the dual-pulse spacing decreases as the external ASE power increases. This is actually opposite to the case of intracavity scheme that starts from the smallest spacing. The standard deviation of the stationary dual-pulse spacing over 20,000 frames exhibits a decreasing trend as the ASE power increases. It implies that the fluctuated force becomes weaker as the ASE power increases, which is opposite to the case via tuning intracavity pump power, and thus the dual-pulse become more stable. It is also noticed that the minimum pulse spacing is about 806 ps at an injected ASE power of 403 μW, which is nearly the same as that of Fig. 3(b). It should be emphasized that, further increasing the ASE power would reduce the stability or even disrupt the mode-locking operation, which is because that the noisy nature of ASE can induce excessive timing perturbation to the coexisting pulses, on the other hand it partially consumes the population inversion of the gain medium that results in insufficient gain for mode-locking sustaining. To illustrate this effect, Figs. 4(d) and 4(e) show the dual-pulse spacing evolution at the ASE powers of 351 μW (i.e., a normal ASE injection) and 1660 μW (i.e., an excessive case), respectively. It is clear that, even though they have similar pulse spacing on average, the latter case exhibits obvious pulse-spacing turbulence, i.e., a larger timing jitter. This phenomenon has also been studied for the ultra-long-distance soliton transmission in optical communication systems [34], and it is found that the random-walk (i.e., Gordon-Haus effect [35]) arising from the noisy perturbation can result in the variation of central wavelength of optical pulses, which consequently exhibits as a timing jitter. Actually, the dual-pulse circulating inside the fiber cavity is equivalent to an ultra-long-distance propagation, which also involves periodic losses and amplifications.

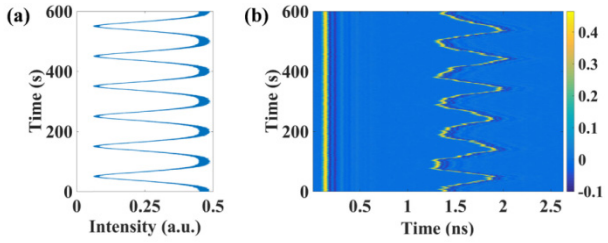

Fig. 5. Pulse-spacing modulation. (a) The pattern of modulated ASE signal. (b) Pulse spacing evolution.

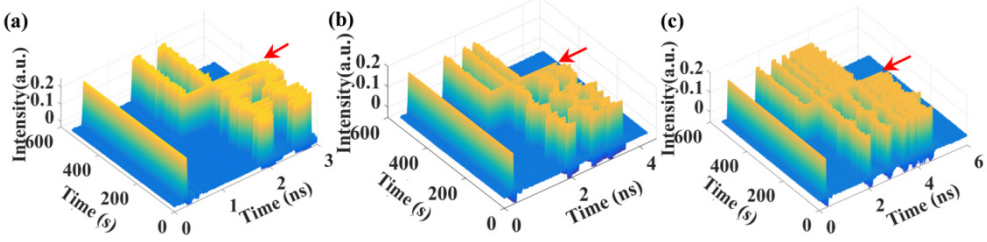

Fig. 6. The pulse evolutions after ASE injection in the cases of three pulses (a), four pulses (b) and ten pulses (c). The red arrows indicate the starting point of ASE injection.

Optics EXPRESS

To further show the flexibility of the dual-pulse spacing control through external ASE injection, we perform dual-pulse spacing modulation by injecting an intensity-modulated ASE. As shown in Fig. 5(a), the intensity of ASE was modulated via the AM at 10 mHz. Figure 5(b) shows the evolution of pulse spacing. It is clear that the pulse spacing was correspondingly modulated. Indeed, a faster modulation frequency is prevented by the relatively-long stabilization time of pulse relocation. Finally, the external ASE injection was also studied for cases with more coexisting pulses. Figures 6(a)-6(c) respectively show the pulse spacing evolutions for three, four and ten pulses. It is clear that the overall pulse distribution is globally shrunk after the ASE injection. It is interesting to point out that, a coexisting nonsoliton component can globally control the relative speeds between those pulses in this work. However, this finding intuitively differs from that of Ref [36]: coexisting solitons would experience different local perturbations and therefore have different central frequency shifts, i.e., resulting in different speeds, when an unstable CW component coexists. This implies that, although it is not the main focus of this work, more efforts are required to fully understand the physical mechanism behind the soliton interaction with different coexisting components (either coherent or incoherent ones) in a dissipative nonlinear system. On the other hand, it actually shows a potential method of optical manipulation on those widely observed soliton rain [20] and soliton molecules [37] in the multipulse mode-locking, which is a hot topic in recent years, particularly for nonlinear physics studies.

5. Conclusion and discussion

In conclusion, we experimentally demonstrated an all-optical pulse-spacing manipulation in a passively mode-locked multipulse fiber laser by both intracavity pump power tuning and external ASE injection. The findings cannot only pave the way for achieving remarkably more stable multipulse pattern, but also provide efficient methods to modulate the pulse-spacing in a passively free-running mode-locked system. Indeed, the current schemes of either external nonsoliton ASE or intracavity continuous-wave pump controlling are relatively global. For a more localized control, the external ASE source can be replaced by a synchronized single-pulse excitation, which thus can produce a localized acoustic wave through electrostriction [38]. It is an effect that the electric field of injected single-pulse can deform the optical fiber and thus generate an acoustic wave, which results in a small time-varying change of refractive index. In this way, the nearby pulse (within ~1.0 ns) can experience a small shifting of center wavelength, and thus speed up or slow down by control the external pulse delay [39]. Instead of externally generating a synchronized single-pulse pattern, it can be obtained through intensity-modulating the optical signal extracting from the under-controlled mode-locked fiber cavity, with the assistance of arbitrary waveform generators (AWGs). Consequently, the efforts made in this work can open new horizons for the active control of a free-running passively mode-locked nonlinear system.

Funding

Research Grants Council of the Hong Kong Special Administrative Region, China (Project Nos. HKU 17205215, HKU 17208414, and CityU T42-103/16-N) and National Natural Science Foundation of China (N_HKU712/16); Innovation and Technology Fund (GHP/050/14GD); and University Development Fund of HKU.